Progress In Electromagnetics Research Letters, Vol. 113, 101–111, 2023

Design of Wideband Circularly Polarized Filtering Antenna with High Frequency Selectivity and Gain Flatness

Zimeng Zhao, Hongmei Liu*, Junhao Ren, Zhongbao Wang, and Shaojun Fang

Abstract—In the paper, a wideband circularly polarized (CP) filtering antenna is proposed, which is composed of four bent Vivaldi elements excited with sequential-rotated feeding technique. Since the Vivaldi element has the advantages of high gain and wide bandwidth, it is selected as the radiation element. On this basis, two cross slots are etched on the Vivaldi antenna to increase the gain at lower frequency band, and bent method which has less effect on the overall performance is applied for lowing the profile of the antenna. To realize filtering characteristic, the quadrature four-feed network consisting of one modified miniaturized filtering rat race coupler (FRC) and two compact wideband quadrature couplers is utilized as the sequential-rotated feeding for the Vivaldi elements. Design procedures of the Vivaldi antenna, the modified filtering FRC, and the quadrature four-feed network are given. For validation, a prototype is fabricated and measured. Results show that more than 60% fractional bandwidth (FBW) is achieved under the criterions of more than 10 dB return loss and less than 3 dB axial ratio. Within the AR bandwidth, the gain is in the range of 7.5 dBic $\sim$ 10.1 dBic. Out of the operation band, the gain sharply decreases to be lower than 5 dBic with a rectangle coefficient ($|\text{Normalized Gain}_{-10\text{-dB}}/\text{Gain}_{0\text{-dB}}|$) of 1.25, which indicates good filtering performance.

1. INTRODUCTION

Circularly polarized (CP) antennas [1, 2] are widely used in satellite communications, radio frequency identification (RFID), mobile communication systems, and wireless sensor networks due to their abilities to resist multipath effects and polarization mismatch, resulting in improved signal quality and reliability. At present, the researches on CP antenna include wideband design, high gain, wide beam, etc. To achieve wideband operation, the commonly used structures include slot antennas [3, 4], spiral antennas [5, 6], aperture antennas [7, 8], and crossed dipoles [9, 10].

In addition to the above studies, filtering characteristics are often integrated into the antenna to suppress out-of-band interference signals and increase integration. In [11], a single-layer CP antenna with filtering response introduced by four thin microstrip stubs and four shorting pins is proposed. It can realize the bandpass filtering function without requiring an external filter. However, the 3-dB axial ratio (AR) bandwidth is only 4.1%, which limits the application. In [12], a high-gain CP filtering stacked patch antenna with independently controllable radiation nulls is designed, where the CP bandwidth is 8.2%. However, adding a stacked patch still cannot expand the CP bandwidth of the antenna obviously. In [13], a compact filtering patch antenna is excited with a fork-shaped line and two half-wavelength strips. On the basis, a CP two element filtering array is designed which has a 3-dB AR bandwidth of 11.4%. However, the lateral dimension is doubled by forming the array. Besides, the bandwidths of reported filtering CP antennas are all less than 15%, which is unsuitable for wideband applications.

Recently, several methods have been presented to expand the AR bandwidth of the filtering CP antennas. In [14], a wideband filtering quadrature coupler based on a snow flake shaped patch and

Received 29 August 2023, Accepted 2 November 2023, Scheduled 13 November 2023
* Corresponding author: Hongmei Liu (lhm323@dlmu.edu.cn).
The authors are with the School of Information Science and Technology, Dalian Maritime University, Dalian 116026, Liaoning, China.

quarter wavelength coupled line sections are proposed as the feeding network of a dielectric resonator antenna. The measured AR bandwidth reaches 27.8%. In [15], the wideband filtering response is introduced by interdigital coupling line feed on an integrated substrate gap waveguide transmission line. Although the bandwidth for 10-dB return loss is extended to 35.06%, the 3-dB AR bandwidth is only 10%. In [16], to achieve a wide AR bandwidth, a parasitic patch with two diagonal slots is loaded on the top of a chamfered patch excited by double Y-shaped slots. As a result, the 3-dB AR bandwidth of 47.3% is realized. However, the gain flatness and frequency selectivity are poor.

In this paper, a wideband CP filtering antenna with high frequency selectivity and gain flatness is proposed. By using the bent Vivaldi elements, high gain and wide bandwidth can be obtained with low profile. Besides, the gain at lower frequency band is increased by inserting two cross-slots. For filtering purpose, the quadrature four-feed network consisting of one modified miniaturized filtering rat race coupler (FRC) and two compact wideband quadrature couplers is utilized as the sequential-rotated feeding for the Vivaldi elements. For validation, a prototype is fabricated and measured. Measurement results show that the prototype has an overlapped fractional bandwidth (FBW) of 60% under the criterion of 10-dB return loss and 3-dB AR, while the gain is in the range of 7.5 dBic $\sim$ 10.1 dBic within the AR bandwidth. Besides, the rectangle coefficient ($|\text{Normalized Gain}_{-10\text{-dB}}/\text{Gain}_{0\text{-dB}}|$) is 1.25, and the out-of-band gain is lower than -5 dBic, which demonstrates good filtering responses.

2. ANTENNA CONFIGURATION AND DESIGN PROCEDURE

2.1. Configuration of the Wideband Filtering CP Antenna

Figure 1 displays the structure of the proposed filtering CP antenna, which is composed of four bent Vivaldi elements with sequential-rotated feeding. Since Vivaldi structure has the characteristics of wideband and prominent radiation, it is applied as a radiator. Besides, a pair of cross slots are etched, and curved metal portions are cut out from the antenna to reduce size and achieve high gain at lower

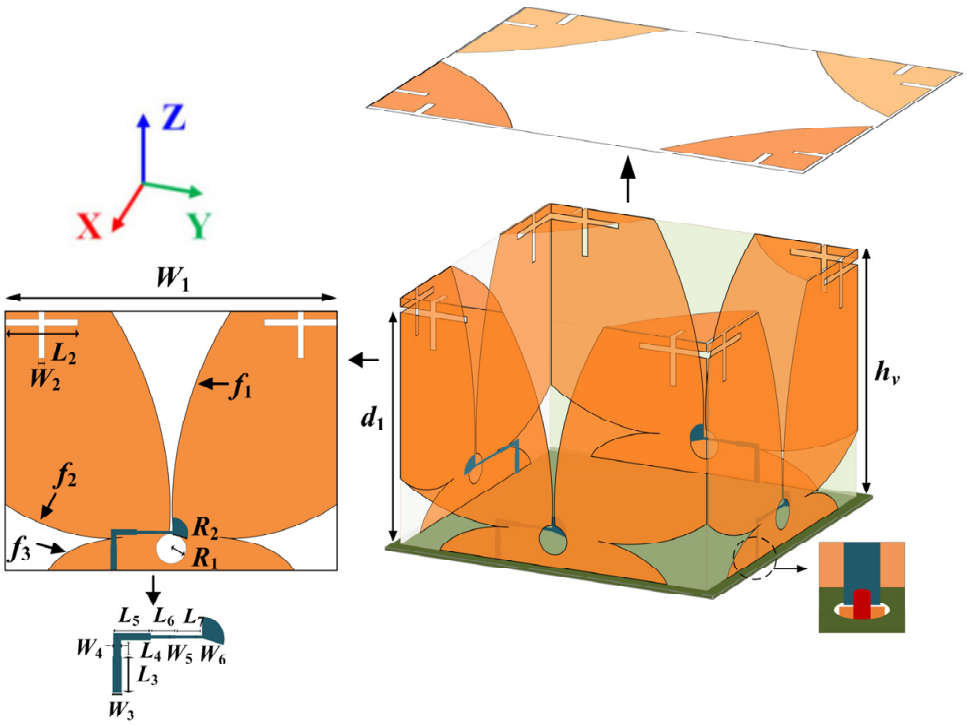

Figure 1. Configuration of the proposed wideband antenna. ($W_1 = 159$ mm, $W_2 = 2.8$ mm, $L_2 = 34$ mm, $W_3 = 2.9$ mm, $L_3 = 12$ mm, $W_4 = 2.5$ mm, $L_4 = 5.9$ mm, $W_5 = 1.45$ mm, $L_5 = 12$ mm, $W_6 = 1.3$ mm, $L_6 = 8$ mm, $L_7 = 8.5$ mm, $h_v = 120.5$ mm, $d_1 = 94$ mm, $R_1 = 7$ mm, $R_2 = 7.1$ mm).

frequency band. For further miniaturization, bent structure is used for the Vivaldi antenna. Equation (1) gives the functions for plotting the curves of f_1, f_2, and f_3 [17]. It is noted that the variable a in (1) determines the position of the curves which is related to the selected coordinate system. In this design, variable a for f_1 is along the z direction, and changes from 0 to 155 mm, while variables a for f_2 and f_3 are both along the x direction, where the variation ranges are -77.5 mm ~ -30.5 mm and -60 mm ~ -30.5 mm, respectively.

$$f_{1\_curve} = 3.93\mathrm{e}^{19.2a} - 0.0033 \tag{1a}$$

$$f_{2\_curve} = -5133\mathrm{e}^{230a} + 0.012\mathrm{e}^{-91a} \tag{1b}$$

$$f_{3\_curve} = \left(1.28 \times 10^{13}\right)\mathrm{e}^{946a} - 0.133\mathrm{e}^{-95a} \tag{1c}$$

A filtering quadrature four-feed network is utilized as the sequential-rotated feeding, which is located on the lower surface of the antenna. Copper columns are used to connect the feeding network with the four bent Vivaldi elements, as shown in Fig. 1. Fig. 2 gives the structure of the filtering quadrature four-feed network. It is composed of one modified miniaturized filtering race coupler (FRC) and two compact wideband quadrature couplers. Here, the modification of the FRC is based on the original design proposed in [18], where size reduction is obtained. Besides, the quadrature coupler which is composed of an inductor loaded coupled line and open-ended stubs is applied for achieving both wideband and small size [19]. In the following, the detailed designs of the bent Vivaldi elements and filtering quadrature four-feed network are introduced respectively.

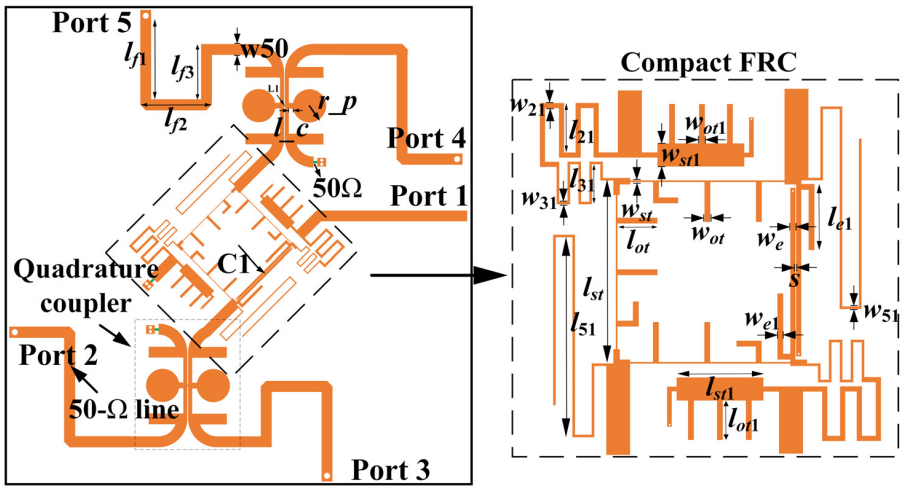

Figure 2. Structure of the filtering quadrature four-feed network. ($W_{st} = 0.25$ mm, $L_{st} = 24$ mm, $W_{ot} = 0.9$ mm, $L_{ot} = 6.34$ mm, $W_{st1} = 3.6$ mm, $L_{st1} = 13.5$ mm, $W_{ot1} = 0.9$ mm, $L_{ot1} = 6.2$ mm, $W_{21} = 0.8$ mm, $L_{21} = 8.5$ mm, $W_{31} = 0.38$ mm, $L_{31} = 5.78$ mm, $W_{51} = 0.4$ mm, $L_{51} = 31.5$ mm, $W_e = 0.8$ mm, $S = 0.19$ mm, $W_{e1} = 0.9$ mm, $L_{e1} = 9.4$ mm, $l_{f1} = 34.7$ mm, $l_{f2} = 21$ mm, $l_{f3} = 18.9$ mm, $W_{50} = 3.73$ mm, $l\_c = 2$ mm, $r\_p = 5.7$ mm).

2.2. Design of the Antenna Based on Bent Vivaldi Elements

Figure 3 shows design evolutions of the proposed antenna. The corresponding performances are shown in Fig. 4. The initial structure starts from Ant. 1 where a typical Vivaldi antenna is designed. To increase the gain at lower frequency band, two cross slots are etched on the Vivaldi antenna. It is seen in Fig. 4 that the gain of Ant. 2 at lower frequency band is obviously improved compare with Ant. 1, while the bandwidth for 10-dB impedance matching is nearly unchanged. On this basis, Ant. 2 is split along the bend line, and the upper part is folded and formed into a bent Vivaldi antenna with the lower part, which results in Ant. 3. This operation can accomplish antenna miniaturization and reduce the antenna height by 31.1%. As seen in Fig. 4, the bending process has small effect on the impedance

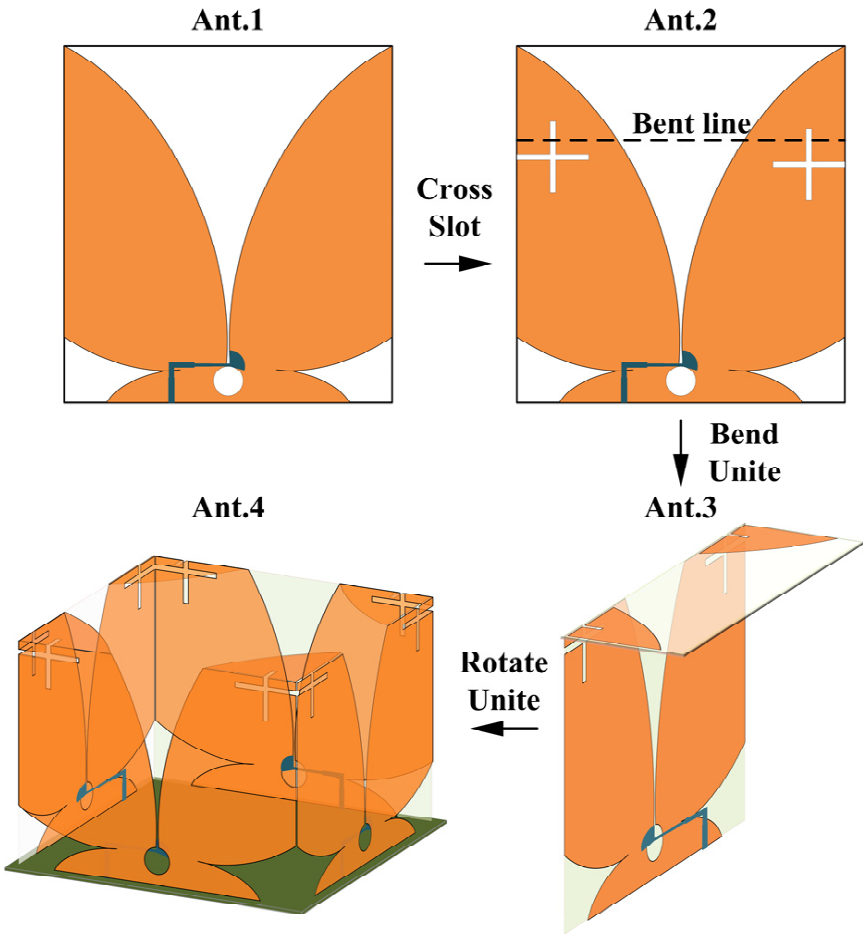

Figure 3. Evolutions of the proposed antenna.

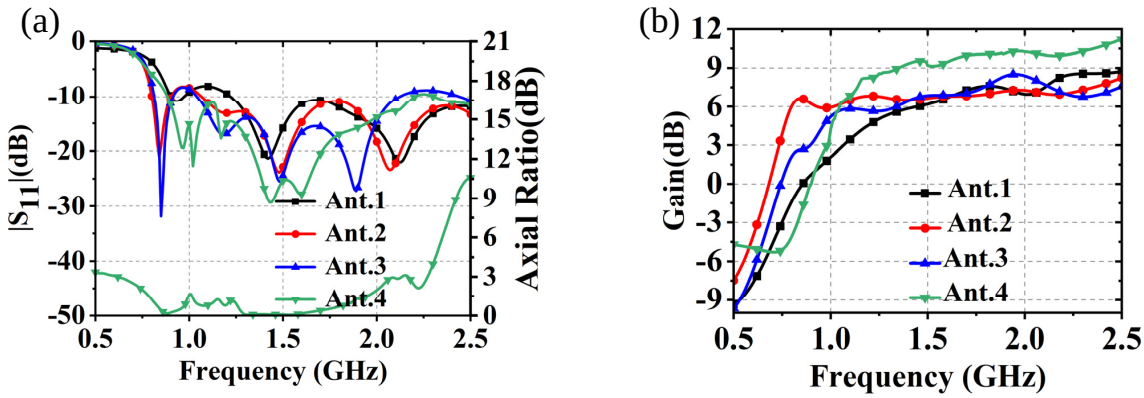

Figure 4. Simulated results of the four evolutions. (a) $|S_{11}|$ and AR. (b) Gain.

matching and gain of the antenna. Finally, the four bent Vivaldi elements are rotated by 90° in turn and then connected to each other to construct a CP antenna (Ant. 4), where the sequential feeding approach is adopted to obtain CP radiation. It is noted that the bending parts for the adjacent elements are overlapped. As can be seen in Fig. 4, an impedance bandwidth of 94.3% (0.88 ∼ 2.20 GHz) is obtained for Ant. 4 under the criterion of 10-dB return loss, while from 1.05 GHz to 2.1 GHz, the AR is less than 3 dB with a realized gain within 6.3 dBic ∼ 11.1 dBic.

2.3. Design of the Filtering Quadrature Four-Feed Network

Figure 5 shows the schematic of the proposed filtering quadrature four-feed network. It is composed of one modified miniaturized wideband filtering FRC and two wideband quadrature couplers, where the couplers are connected to the out-of-phase ports of the FRC. According to [19], the parameters of a 3-dB compact wideband coupler can be calculated, where $C_1 = 3.1\,\text{pF}$, $L_1 = 4.9\,\text{nH}$, $Z_{2e} = 106.6\,\Omega$, $Z_{2o} = 46\,\Omega$, $Z_2 = 36\,\Omega$, $\theta_1 = 57.5°$, and $\theta_2 = 25.3°$. In the following, the design of the modified miniaturized wideband filtering rat-race coupler is mainly introduced. The original structure of the FRC is proposed in [18], which has the merits of filtering response, wide bandwidth, and flat output distributions. However, the FRC in [18] is large in size and not suitable for constructing the feed network of the proposed CP antenna. Thus, modification is performed to reduce the size.

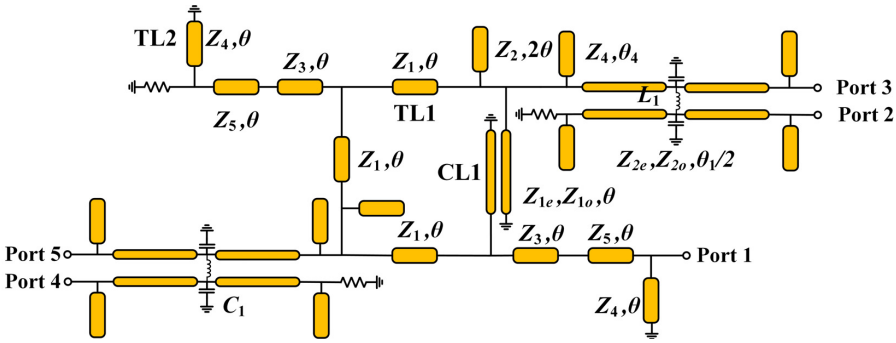

Figure 5. The schematic of the proposed filtering quadrature four-feed network.

In order to reduce the size of FRC, as well as keep output ports phase flatness, the TL1s (Z_1, θ) and TL2s (Z_4, θ) are replaced by three-period stepped-impedance T-type (SMT) TL, where the schematic is shown in Fig. 6(a). In addition, the CL1 (Z_{1e}, Z_{1o}, θ) is replaced by a short-circuited CL loaded with open-ended stubs and one capacitor, as shown in Fig. 6(b). Using equivalent theory, the relations between the TL1/2 and its modified miniaturized structure are listed in (2).

$$Z_{st} = Z_2 \frac{\tan\dfrac{\theta_2}{6}}{\tan\dfrac{\theta_{st}}{2}} \tag{2a}$$

$$Y_{ot} = \frac{2}{Z_{st}} \cdot \frac{Z_{st} - Z_2 \cot\dfrac{\theta_2}{6}\tan\dfrac{\theta_{st}}{2}}{Z_{st}\tan\dfrac{\theta_{st}}{2} + Z_2\cot\dfrac{\theta_2}{6}} \cdot \cot\theta_{ot} \tag{2b}$$

$$Z_2 = Z_a\sqrt{\frac{Z_a^2\tan^2\theta_a - Z_0^2}{Z_0^2\tan^2\theta_a - Z_a^2}} \tag{2c}$$

$$\theta_2 = 2\left(\tan^{-1}\sqrt{\frac{(Z_0 - Z_a\tan\theta_a)(Z_a - Z_0\tan\theta_a)}{(Z_0 + Z_a\tan\theta_a)(Z_a + Z_0\tan\theta_a)}}\right) \tag{2d}$$

Here, the values of Z_a and θ_a with replacing TL1 are set to $120\,\Omega$ and 5°. The values of Z_a and θ_a with replacing TL2 are set to $90\,\Omega$ and 10°. According to Fig. 6(b), by multiplying the matrices of capacitor-loaded short-circuited CL $[A_{o2}]$ with the open-ended stub $[A_{o1}]$, the $ABCD$ matrix $[A_o]$ of short-circuited CL loaded with open-ended stubs and one capacitor is derived.

$$[A_o] = [A_{o1}] \cdot [A_{o2}] \cdot [A_{o1}] = \begin{bmatrix} A & B \\ C & D \end{bmatrix} \tag{3a}$$

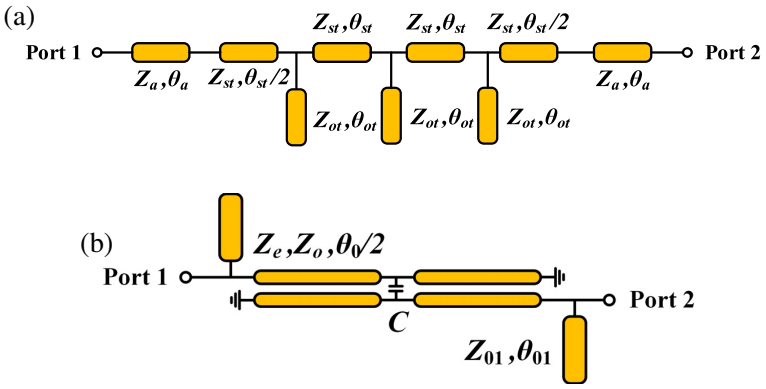

Figure 6. Equivalent circuits of (a) TL1 and TL3. (b) CL1.

where

$$A = D = \frac{Z_o(\tan\theta_0 - 2\cot\theta_0)(1-\omega CZ_o\tan\theta_0) + Z_e\tan\dfrac{\theta_{01}}{2}(\omega CZ_o + \tan\theta_0)}{Z_o\tan\theta_0(1-\omega CZ_o\tan\theta_0) - Z_o(\omega CZ_o+\tan\theta_0)} + \frac{\tan\dfrac{\theta_{01}}{2}Z_oZ_e(1-\omega CZ_o\tan\theta_0)}{Z_{01}\left[Z_o\tan\theta_0(1-\omega CZ_o\tan\theta_0) - Z_e(\omega CZ_o+\tan\theta_0)\right]} \tag{3b}$$

$$B = \frac{\mathrm{j}Z_oZ_e(1-\omega CZ_o\tan\theta_0)}{Z_o\tan\theta_0(1-\omega CZ_o\tan\theta_0) - Z_e(\omega CZ_o+\tan\theta_0)} \tag{3c}$$

$$C = \frac{2\tan\dfrac{\theta_{01}}{2}\left[Z_o(\tan\theta_0 - 2\cot\theta_0)(1-\omega CZ_o\tan\theta_0) + Z_e(\omega CZ_o+\tan\theta_0)\right]}{jZ_{01}Z_o\left[\tan\theta_0(1-\omega CZ_o\tan\theta_0) - (\omega CZ_o+\tan\theta_0)\right]} + \frac{\left(\tan^2\dfrac{\theta_{01}}{2} - Z_{01}^2\right)\left[Z_oZ_e(1-\omega CZ_o\tan\theta_0)\right]}{jZ_{01}^2\left[Z_o\tan\theta_0(1-\omega CZ_o\tan\theta_0) - Z_e(\omega CZ_o+\tan\theta_0)\right]} \tag{3d}$$

The $ABCD$ matrix of the CL1 can be expressed as

$$[A_{c1}] = \begin{bmatrix} A_c & B_c \\ C_c & D_c \end{bmatrix} \tag{4a}$$

$$A_c = D_c = \frac{\cot\theta/Z_{1e} + \cot\theta/Z_{1o}}{\csc\theta/Z_{1e} - \csc\theta/Z_{1o}} \tag{4b}$$

$$B_c = \frac{2j}{\csc\theta/Z_{1e} - \csc\theta/Z_{1o}} \tag{4c}$$

$$C_c = \frac{1/Z_{1e}^2 + 1/Z_{1o}^2 - 2\left(\cot^2\theta + \csc^2\theta\right)/(Z_{1e}Z_{1o})}{j/2(\csc\theta/Z_{1e} - \csc\theta/Z_{1o})} \tag{4d}$$

By equalizing the matrix parameters in $[A_o]$ and $[A_{c1}]$, the replacement of CL1 by the short-circuited CL loaded with open-ended stubs can be performed. Table 1 illustrates the calculated circuit parameters of the modified FRC.

Figure 7 shows the theory results of the designed modified FRC. It is seen that under the criterion of $|S_{11}| < -10\,\mathrm{dB}$, the relative bandwidths for ports 1 and 4 excitations are 67% and 54%, respectively. In the whole shown frequency band, the isolations of the FRC are both larger than 20 dB. Besides, in the bandwidth of 1.16 GHz to 1.66 GHz (38%), the output ports amplitude imbalances (APIs) are less than 0.5 dB, and the phase difference (PD) errors are within $\pm5^\circ$ for both ports 1 and 4 excitations.

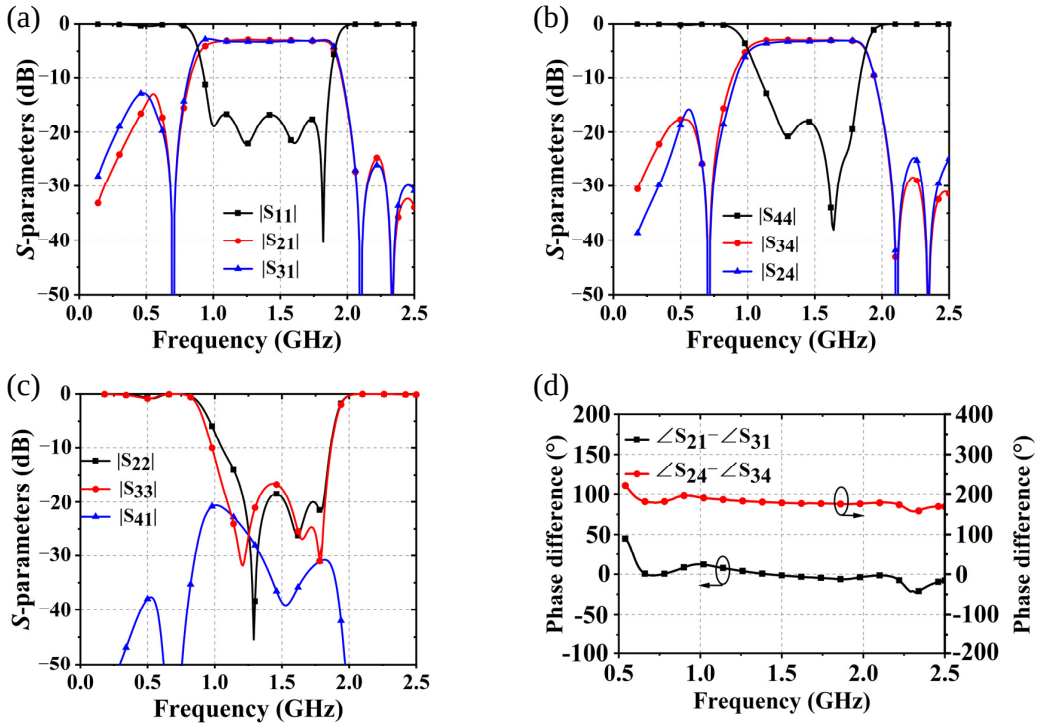

Figure 7. Theory frequency responses of the modified FRC. (a) $|S_{11}|$, $|S_{21}|$ and $|S_{31}|$. (b) $|S_{44}|$, $|S_{24}|$ and $|S_{34}|$. (c) $|S_{22}|$, $|S_{33}|$ and $|S_{41}|$. (d) $\angle S_{21} - \angle S_{31}$, $\angle S_{24} - \angle S_{34}$.

Table 1. The calculated parameters of the designed FRC.

Z_a (Ω)	Z_{st} (Ω)	Z_{ot} (Ω)	Z_{a1} (Ω)	Z_{st1} (Ω)	Z_{ot1} (Ω)	C (pF)
120	146	100	91.5	93	28	1.06
Z_{01} (Ω)	Z_2 (Ω)	Z_3 (Ω)	Z_5 (Ω)	Z_e (Ω)	Z_o (Ω)	θ_a (°)
116.4	90	136	92	161	67	5.4
θ_{st} (°)	θ_{ot} (°)	θ_{a1} (°)	θ_{st1} (°)	θ_{ot1} (°)	θ_0 (°)	θ_{01} (°)
17.5	14.9	10.32	7.86	12.6	46.6	31

When the modified FRC is combined with the 3-dB compact wideband coupler, a quadrature four-feed filtering network is constructed, as shown in Fig. 2. It is noted that a size reduction of 57.4% is obtained, comparing the modified FRC with the original one in [18]. Fig. 8 shows the simulated frequency responses of the four-feed network. It is seen that the return loss is larger than 10 dB from 0.99 GHz to 1.8 GHz, yielding a relative bandwidth of 62.1%. While the output port distributions are 6.2 ± 0.7 dB, and the $\pm 5°$ phase inaccuracy is expected in the bandwidth of 1.16 GHz to 1.8 GHz (46%). For 10-dB out-of-band rejection, the simulated bandwidth is extended to 3.16 GHz ($2.26 f_0$). Besides, the 3-dB FBW is from 0.92 GHz to 1.86 GHz, and the rectangular coefficient ($|\mathrm{BW}_{30\,\mathrm{dB}}/\mathrm{BW}_{6\,\mathrm{dB}}|$) is 1.35.

3. EXPERIMENTAL RESULTS

For demonstration, the designed antenna and feed network are fabricated on an F4BM substrate. ($\varepsilon_r = 3$, $\tan\delta = 0.001$, $h = 1.5$ mm) and integrated, as shown in Fig. 9. The overall dimension of the antenna is 170 mm × 170 mm × 122 mm. The simulated and measured results of $|S_{11}|$, AR, and gain

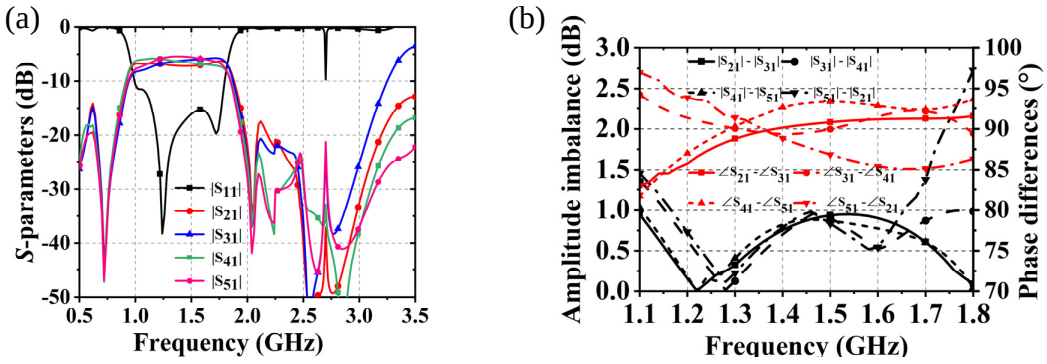

Figure 8. Simulated results of the final feed network (a) S-parameters. (b) Amplitude imbalance and phase difference.

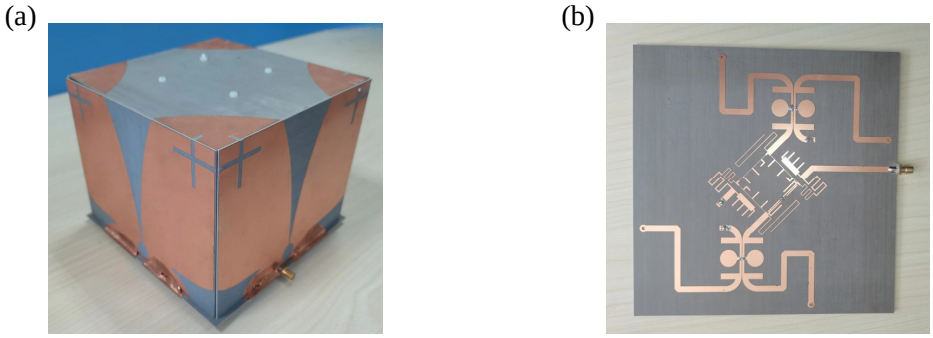

Figure 9. Photograph of the fabricated antenna (a) 3D view. (b) Bottom view.

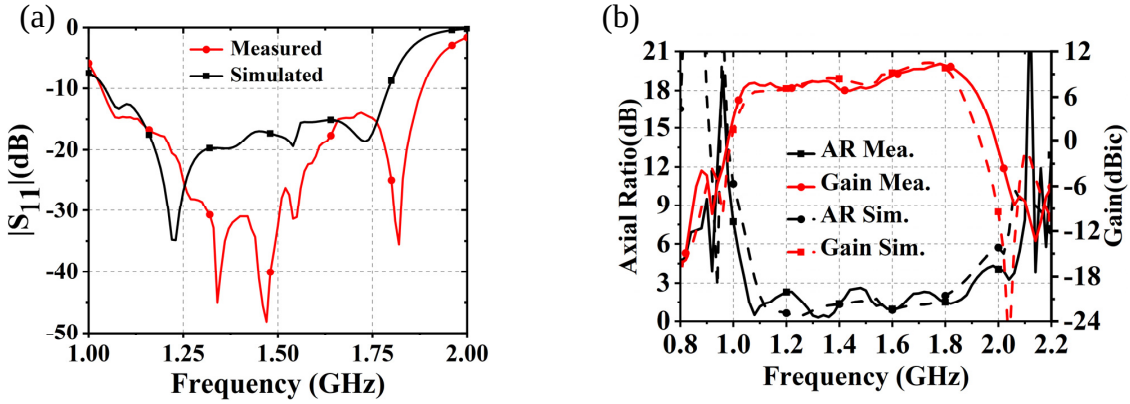

Figure 10. Simulated and measured results of the fabricated antenna (a) $|S_{11}|$. (b) AR and gain.

of the fabricated antenna are shown in Fig. 10. As can be seen, the measured FBW under the criterion of 10-dB return loss is in the range of 1.04 GHz $\sim$ 1.88 GHz (60%), and the 3-dB AR bandwidth is from 1.06 GHz to 1.9 GHz (60%). In AR bandwidth, the gain is in the range of 7.5 dBic $\sim$ 10.1 dBic, which has flatness. On the other hand, out of the operation band, the gain is sharply reduced to be lower than 5 dBic, which indicates good out-of-band rejection. The measured RC of the fabricated antenna is 1.25 under the criterion of |Normalized $\text{Gain}_{-10\text{-dB}}/\text{Gain}_{0\text{-dB}}$|. Fig. 11 shows simulated and measured radiation patterns of the proposed antenna in which the radiation fields of right hand circular polarization (RHCP) are more than 15 dB stronger than that of the left hand circular polarization (LHCP) in the main direction with symmetric radiation patterns.

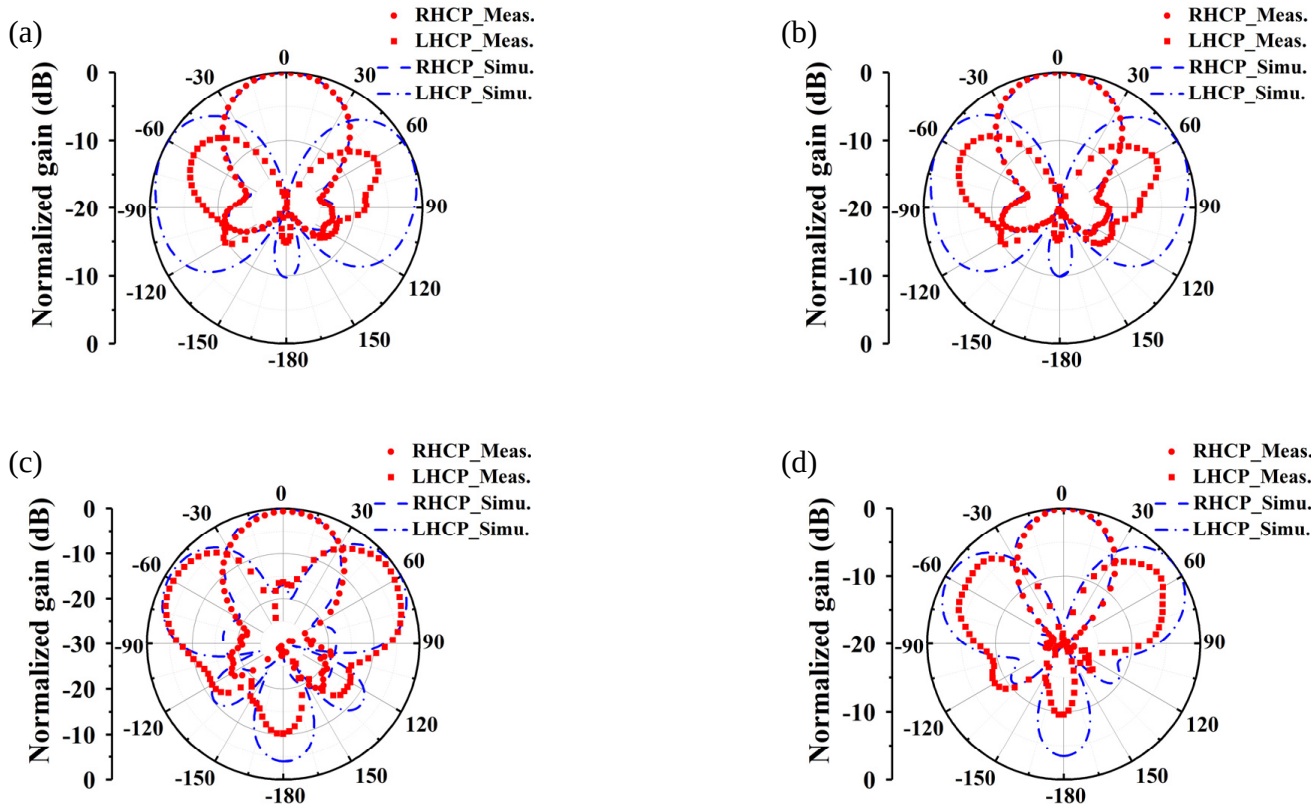

Figure 11. Simulated and measured radiation patterns of the fabricated antenna (a) 1.207 GHz. (b) 1.228 GHz. (c) 1.561 GHz. (d) 1.602 GHz.

Table 2. Performance comparisons between the designed and CP filtering antenna.

	10-dB FBW (%)	ARBW (%)	RC	Out-of-band suppression (dB)	Gain[a] (dBic)	Size (λ_0^3)
[11]	4.5%	5.3%	1.83	20	5–8.3	$0.5 \times 0.5 \times 0.02$
[12]	15.2%	8.2%	1.96	22	4.5–7	$0.52 \times 0.52 \times 0.06$
[13]	11.4%	11.4%	1.38	21.43	7–10.7	$1.54 \times 0.88 \times 0.035$
[15]	35.06%	10%	1.45	14.4	6–8	$0.55 \times 0.55 \times 0.05$
[16]	59.4%	47.3%	1.85	15	5–9	—
This work	**60%**	**60%**	**1.25**	**14**	**7.5–10.1**	$\mathbf{0.74 \times 0.74 \times 0.56}$

[a] Gain in the AR bandwidth. RC = |Normalized $\text{Gain}_{-10\text{-dB}}/\text{Gain}_{0\text{-dB}}$|. λ_0 is the wave length at the lowest operating frequency.

Table 2 compares the performances of presented antenna with the reported filtering CP antennas. Though the antennas in [11–13] have good frequency suppression levels, they all show narrow FBW and AR bandwidths ($< 15\%$). The antenna in [15] also has narrow AR bandwidth. Although an extended bandwidth is observed for the CP antenna in [16], the frequency selectivity and gain flatness are worse than the proposed antenna. In summary, the proposed CP filtering antenna has the merits of wide bandwidth, high gain, good filtering characteristic, and gain flatness feature, which can be used for wideband CP applications.

4. CONCLUSION

In this paper, the design of a wideband filtering CP antenna is performed based on the four bent Vivaldi elements excited with sequential-rotated feeding technique. The Vivaldi element is used as a radiator due to the advantages of high gain and wide bandwidth. Besides, two cross slots are etched, and bent method is used to increase the gain at lower frequency band and decrease the profile of the antenna, respectively. Filtering response is obtained by using the quadrature four-feed network where the essential component is the modified FRC with filtering characteristic and small size. A prototype is fabricated. Results show that the proposed antenna has the advantages of wide bandwidth, high gain, good frequency selectivity, and gain flatness feature compared with other filtering CP antennas, which can be a good candidate in wideband CP applications.

ACKNOWLEDGMENT

This work was supported in part by the National Natural Science Foundation of China under Grant 51809030, in part by the Liaoning Revitalization Talents Program under Grant XLYC2007067, in part by the Young Elite Scientists Sponsorship Program by CAST under Grant 2022QNRC001 and in part by the Fundamental Research Funds for the Central Universities under Grant 3132023246.

REFERENCES

1. Liu, Y., X. Liang, C. Fang, J. Geng, and R. Jin, "A K-band circularly-polarized slot antenna based on L-shaped waveguide cavity," *International Conference on Microwave and Millimeter Wave Technology (ICMMT)*, 1–3, Nanjing, China, May 2021.
2. Soliman, S. A. M., E. M. Eldesouki, A. M. Attiya, A. P. Freundorfer, and Y. M. M. Antar, "Circularly polarized folded reflectarray antenna," *International Microwave and Antenna Symposium (IMAS)*, 36–40, Cairo, Egypt, March 2023.
3. Li, J., H. Shi, H. Li, and A. Zhang, "Quad-band probe-fed stacked annular patch antenna for GNSS applications," *IEEE Antennas Wireless Propag. Lett.*, Vol. 13, 372–375, 2014.
4. Li, X., Y. Li, J. T. Huang, and O. Yang Du, "A cross-slot loaded miniaturized UWB Vivaldi dual-polarized antenna," *International Conference on Microwave and Millimeter Wave Technology (ICMMT)*, 1–3, Nanjing, China, May 2021.
5. Guo, L., P. Zhang, F. Zeng, Z. Zhang, and C. Zhang, "A novel four-arm planar spiral antenna for GNSS application," *IEEE Access*, Vol. 9, 168899–168906, 2021.
6. Zhong, Z.-P. and X. Zhang, "A travelling-wave-fed slot spiral antenna with wide axial-ratio bandwidth and beamwidth for GNSS applications," *IEEE Open Journal Antennas Propag.*, Vol. 2, 578–584, 2021.
7. Zhang, Y.-X., Y.-C. Jiao, Z. Zhang, and S. Feng, "Wideband accurate-out-of-phase-fed circularly polarized array based on penta-mode aperture antenna element with irregular cavity," *IEEE Trans. Antennas Propag.*, Vol. 67, No. 1, 638–642, Jan. 2019.
8. Li, X., R. Ma, H. Cai, Y.-M. Pan, and X. Y. Zhang, "High-gain dual-band aperture-shared CP patch antenna with wide AR beamwidth for Satellite Navigation System," *IEEE Antennas Wireless Propag. Lett.*, Vol. 22, No. 8, 1888–1891, Aug. 2023.
9. Cicchetti, R., V. Cicchetti, A. Faraone, L. Foged, and O. Testa, "A compact high-gain wideband lens Vivaldi antenna for wireless communications and through-the-wall imaging," *IEEE Trans. Antennas Propag.*, Vol. 69, No. 6, 3177–3192, Jun. 2021.
10. Zhang, H., Y. Guo, and G. Wang, "A design of wideband circularly polarized antenna with stable phase center over the whole GNSS bands," *IEEE Antennas Wireless Propag. Lett.*, Vol. 18, No. 12, 2746–2750, Dec. 2019.
11. Yang, W. J., Y. M. Pan, and X. Y. Zhang, "A single-layer low-profile circularly polarized filtering patch antenna," *IEEE Antennas Wireless Propag. Lett.*, Vol. 20, No. 4, 602–606, Apr. 2021.

12. Cheng, G., B. Huang, Z. Huang, and L. Yang, "A high-gain circularly polarized filtering stacked patch antenna," *IEEE Antennas Wireless Propag. Lett.*, Vol. 22, No. 5, 995–999, May 2023.
13. Liu, S., Z. Wang, and Y. Dong, "A compact filtering patch antenna with high suppression level and its CP application," *IEEE Antennas Wireless Propag. Lett.*. Vol. 22, No. 4, 769–773, April 2023.
14. Xiang, B. J., S. Y. Zheng, Y. M. Pan, and Y. X. Li, "Wideband circularly polarized dielectric resonator antenna with bandpass filtering and wide harmonics suppression response," *IEEE Trans. Antennas Propag.*, Vol. 65, No. 4, 2096–2101, April 2017.
15. Zhong, X., D. Shen, L. Zhou, D. You, Q. Lin, and X. Zhang, "Circularly polarized filtering antenna based on integrated substrate gap waveguide," *IEEE MTT-S International Wireless Symposium (IWS)*, 1–3, Nanjing, China, 2021.
16. Wang, J. and Y. Zhang, "Broadband high gain circularly polarized filtering antenna," *IEEE Conference on Antenna Measurements and Applications (CAMA)*, 1–3, Guangzhou, China, 2022.
17. Zhang, K., R. Tan, Z. H. Jiang, Y. Huang, L. Tang, and W. Hong, "A compact, ultrawideband dual-polarized Vivaldi antenna with radar cross section reduction," *IEEE Antennas Wireless Propag. Lett.*, Vol. 21, No. 7, 1323–1327, July 2022.
18. Zhao, Z. M., H. M. Liu, J. H. Ren, Z. B. Wang, and S. J. Fang, "Wideband filtering rat-race coupler with shared triple-mode resonator," *Electronics*, Vol. 12, No. 12, 2023.
19. Liu, H. M., M. Y. Guan, H. X. Zhang, S. J. Fang, and Z. B. Wang, "Compact wideband and harmonic suppressed quadrature coupler using susceptance loaded coupled lines," *Microw. Opt. Technol. Lett.*, Vol. 64, No. 3, 507–514, March 2022.